

Electro-Thermal Analysis of a microheater for aerosol generation application

M.Saberi¹, U.Pelz¹, M.Ghanam¹, T. Bilger¹, A.Jamali¹, E. Baeumker¹, T.Gerach¹, P. Woias¹, F. Goldschmidtboeing¹

¹Institut für Mikrosystemtechnik (IMTEK), Albert-Ludwigs-Universität Freiburg, Freiburg im Breisgau, Germany

Abstract

There is an increasing demand for aerosol devices from E-cigarettes to drug delivery devices with precise dosage[1][2]. This article aims to investigate a silicon microheater performance in a vapor generator device. In order to calculate the amount of vapor production, temperature distribution, and heat loss calculation of the heater a simulation setup was modeled in COMSOL. The 3D setup consists of a rectangular perforated silicon heater which is placed on a wet fiberglass wick material and powered through gold wire bonds to a PCB. The heater chip is mounted inside the PCB using epoxy glue (Figure 2). The simulation implements coupled electrical current, heat transfer, laminar flow physics, and events modules. The electrical current and heat transfer modules are coupled using a joule heating Multiphysics. The electrical input power is controlled based on the temperature of the heater using the events interface. There is also Non-isothermal flow Multiphysics which couples heat transfer and laminar flow module to account for liquid flow and phase change. All domains are manually meshed using mostly hexahedral and prism elements. The amount of vapor produced is about 0.65 mg after 3 seconds with temperature regulation around 270°C. The heat losses to surrounding air via convection and through wire bonds via conduction are negligible, however, most of the heat goes to the liquid and epoxy material. The evaporation starts at 0.1 seconds and is almost linearly increasing by time.

Introduction

A microheater to generate aerosol was fabricated and should be characterized (Figure 1). Besides experimental measurements [3], a simulation model needs to describe the performance of it. The microheater assembly includes a silicon heater, a PCB, and some epoxy glue to mount it on the measurement bench. The size of the heater element is 300x2000x3000 μm and there is no dimension bigger than 10mm in the simulation model. The experimental setup makes it possible to measure electrical power input and vapor weight per usage. However, it does not give an insight into what happens inside the structure.

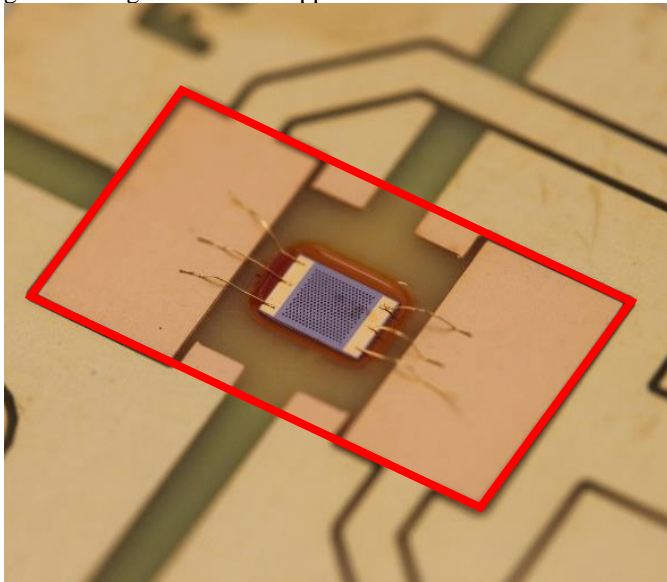


Figure 1 the fabricated heater on PCB – simulation domain in red.

In this paper, the simulation setup is described and the results are discussed.

Goals and assumptions

The objective of the simulation is to get an insight into temperature distribution in the domain, the amount and distribution of vapor in wick material, and heat loss fluxes. It is also desired to check for any temperature violation.

In order to model the system in COMSOL, some assumptions are made (Figure 2). Electrically conductive materials have linear temperature-dependent electrical resistivity. Radiation heat transfer is neglected. Thermal and electrical contacts between materials are ideal. The liquid mixture is considered as

a single material with equivalent properties. Porous media and liquid inside that are supposed to have the same temperature.

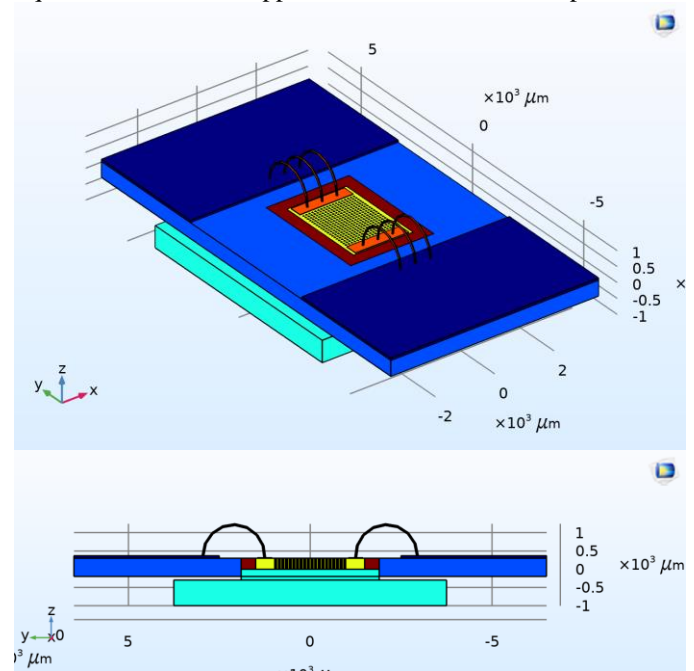


Figure 2 simulation domain in COMSOL software.

Input power ON/OFF state is controlled by the average volume temperature of the heater. The liquid flows inside the wick material by hydraulic force and capillary force is neglected.

Numerical model and governing equations

The numerical model in COMSOL consists of Heat Transfer (HT), Laminar Flow (LF), Electrical Current (EC), and Events (EV) module. The heat transfer module runs all over the domains and considers porous media and phase change material inside the wick material domain. The equations account for conduction and convection heat transfer. The electrical current module only runs through electrically conductive domains which are copper pads on PCB, gold wire bonds, and pads on the heater, as well as the silicon heater element. The laminar flow module only works inside wick material where the liquid flows. It accounts for flow in porous media as well as the hydraulic force due to gravity. The walls have slip condition since the wall effect is negligible inside the fluid domain. In the Events module, there are conditions to turn the electrical terminal boundary condition on or off based on the volume

average temperature of the heater element. This average is calculated while solving using components coupling in the definition section of the software. [4] The Electromagnetic Heating Multiphysics (Joule heating) and Nonisothermal Flow link the heat transfer module to electrical current and laminar flow respectively. The equations are software defaults on these modules and not manipulated with custom codes.

The equations for heat transfer are time transient 3D Cartesian conduction as Equation 1.

$$\rho C_p \frac{\partial T}{\partial t} + \rho C_p u \cdot \nabla T + \nabla \cdot q = Q + Q_{ted} \quad \text{Equation 1}$$

$$q = -k \nabla T$$

Phase change inside wick material uses a weighted average of material properties between the liquid and gas phases. The equation sets are in Equation 2.

$$\rho = \theta_1 \rho_1 + \theta_2 \rho_2$$

$$C_p = \frac{1}{\rho} (\theta_1 \rho_1 C_{p,1} + \theta_2 \rho_2 C_{p,2}) + L_{1 \rightarrow 2} \frac{\partial \alpha_m}{\partial T}$$

$$\alpha_m = \frac{1}{2} \frac{\theta_2 \rho_2 - \theta_1 \rho_1}{\theta_1 \rho_1 + \theta_2 \rho_2} \quad \text{Equation 2}$$

$$k = \theta_1 k_1 + \theta_2 k_2$$

$$\theta_1 + \theta_2 = 1$$

Equations for electrical current are shown as Equation 3.

$$\nabla \cdot J = Q_{j,v}$$

$$J = \sigma E + \frac{\partial D}{\partial t} + J_e \quad \text{Equation 3}$$

$$E = -\nabla v$$

Laminar flow in porous media

$$\rho(u \cdot \nabla)u = \nabla \cdot [-pI + K] + F + \rho g$$

$$\rho \nabla \cdot (u) = 0 \quad \text{Equation 4}$$

$$K = \mu(\nabla u + (\nabla u)^T)$$

All equations come from software documentation and COMSOL discretizes them over them geometry.

A custom mesh was used to describe the geometry because of thin and small sections. The mesh consists of prism and hexahedrons as most of them are created with mesh sweep feature (Figure 3).

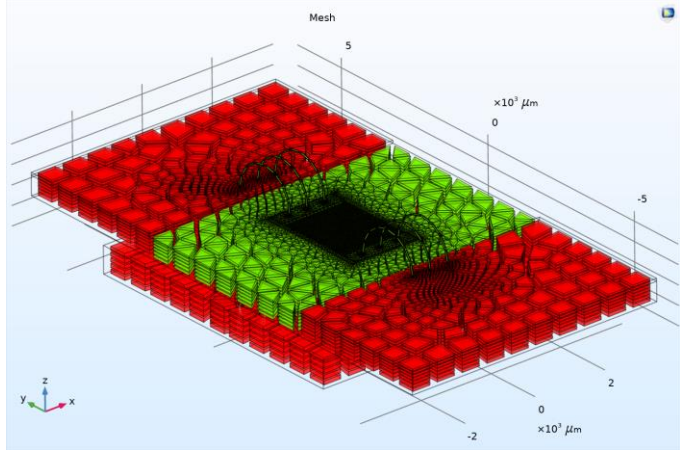


Figure 3 custom mesh, prism elements green, and hexahedrons red.

The study is transient and includes the first 3 seconds of evaporation from the initial rest condition. To have more stable initial conditions, a steady-state study calculates the values just for heat transfer and electrical current without any other modules or Multiphysics enabled.

Boundary and initial condition

All boundary conditions are applied on surfaces as the model is in 3D. Electrical boundary conditions consist of two voltage

terminals of VCC and ground. The VCC terminal switches between zero and 3.7[V] if the temperature of the heater element exceeds 270°. There is pressure type fluid inlet from wick wall sides. Hydrostatic pressure compensation and no back-flow condition is governing the inflow. All holes on top of the heater element have pressure type outflow condition. The gravity reference point is beneath the heater element. Free natural convection is considered on all top surfaces and sidewalls of the PCB are supposed to meet room temperature. Initially, the temperature all over the domain is room temperature. The liquid has zero velocity and the circuit is electrically closed so that we have electrical current.

Material properties

For silicon, copper, FR4, glass fiber, and gold the software built-in material properties were used with minimum modifications. The epoxy and liquid have custom properties.

Table 1: liquid properties

Properties	Value	Unit
Density	1200	kg/m ³
Thermal Conductivity	0.5	W/(m·K)
Thermal Capacity (Specific heat)	2600	J/(K.kg)
Dynamic viscosity	0.0025	Pa·s
Evaporation temperature	210	°C
Specific heat for evaporation (latent heat of vaporization, LV)	840	kJ/kg

Phase change happens at the evaporation temperature of the liquid and the transition temperature is 20°C. Wick porosity is 0.9 and has a permeability of 2.12e-12[m²].

Epoxy properties are also custom ones.

Table 2: epoxy glue properties

Properties	Value	Unit
Density	1300	kg/m ³
Thermal conductivity	1.26	W/(m·K)
Heat capacity at constant pressure	1.4	J/(kg·K)

Simulation results and discussion

The simulation takes approximately 8 hours on an AMD Ryzen ThreadRipper 1950x client with 64GB of system memory when the solver tolerance and event tolerance are set 1e-4 and of 0.01. The first result is the temperature distribution. As in Figure 4, the hottest spot is on the silicon heater which is expected. The next hot component is epoxy.

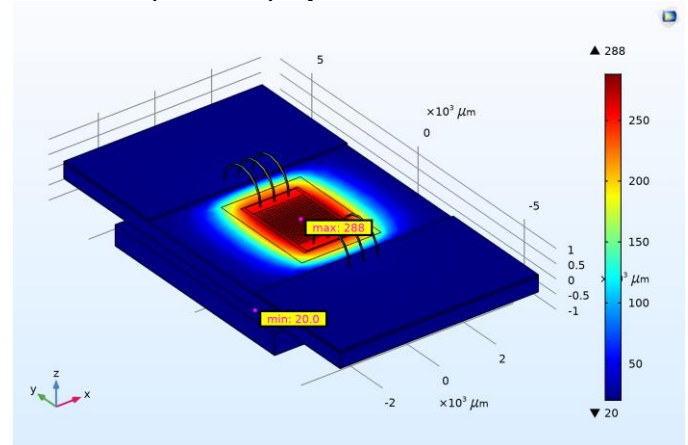


Figure 4 temperature distribution all over domain at t=3s.

The maximum temperature on each component through time is illustrated in Figure 5.

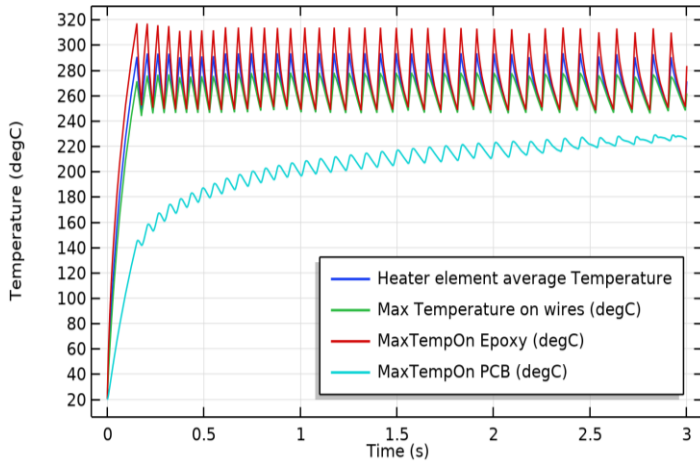


Figure 5 maximum temperature on the heater, PCB, Epoxy, and wires.

The temperature on silicon and gold wire bonds are below the melting point. However, FR4 composite of PCB and epoxy glue experience temperature above their limits. Although the epoxy failure was observed in some of the epoxies on the repetitive evaporation test, no damage was observed on PCB.

Evaporation distribution and amount

Evaporation starts inside the wick at about 0.1 seconds. As the amount of vapor increases inside the wick, its density is decreased and it expands. Expansion leads the gas to be pushed out of the wick domain. Also, the vapor is lighter than the liquid. Then the vapor is pushed outside the wick from heater holes because of hydrostatic pressure from the inlet. The amount of vapor inside the wick Figure 6, however, the outflow is still negligible to be reported. Based on the simulation, there will be 0.65 mg vapor at the end of 3 seconds with a switching temperature of 270°C.

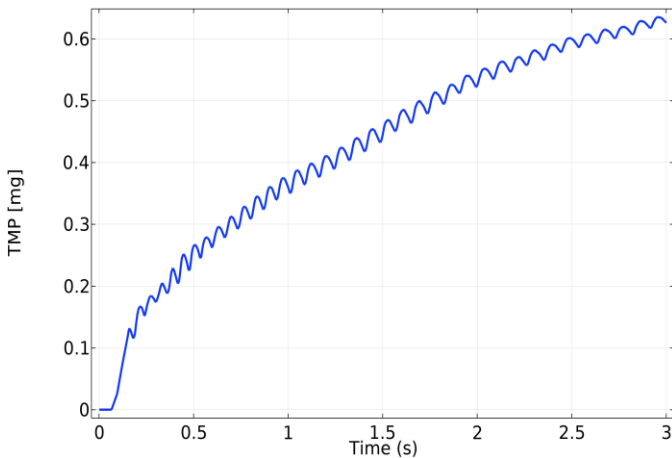


Figure 6 amount of vapor generated inside wick.

The vapor distribution is almost even under the heater, however, the thickness of the vapor layer is higher in the center. The vapor distribution as well as temperature contours inside the sectioned wick material at the end of the simulation is shown in Figure 7. It is visible that the vapor phase (red color) and liquid phase (blue color) split along the contour line of 210°C which is the evaporation temperature.

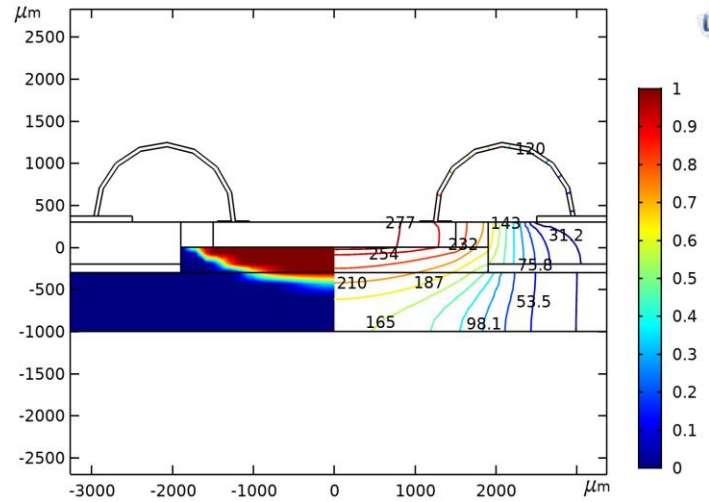


Figure 7 vapor/liquid distribution and temperature in wick, t=3s.

In order to follow the temperature and phase change, a vertical axis in the middle of wick material is considered which starts right beneath the heater and extends till the bottom of the wick. The temperature at different time steps is shown over this vertical line in Figure 8. The dashed line is the evaporation temperature of the liquid and the liquid almost reaches that at 0.06 seconds. At the end of 3 seconds, the temperature in the depth of 400um in the middle of the wick exceeds the evaporation point.

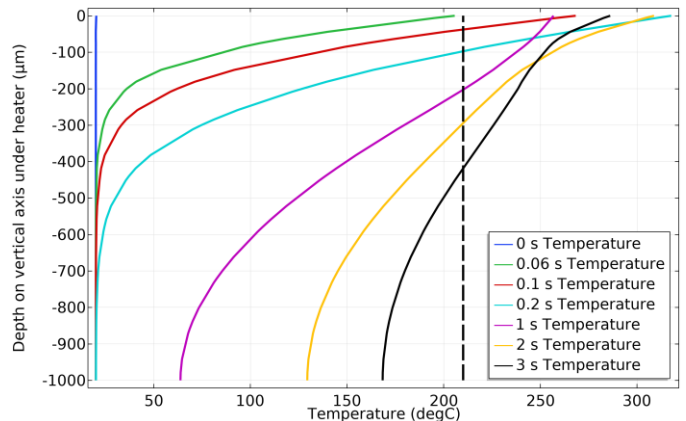


Figure 8 time transient liquid temperature on vertical axis inside wick.

Figure 9 shows the volume fraction of the vapor phase over time and depth of wick better. The vertical axis represents vapor depth and it reaches 300 um at end of the evaporation period.

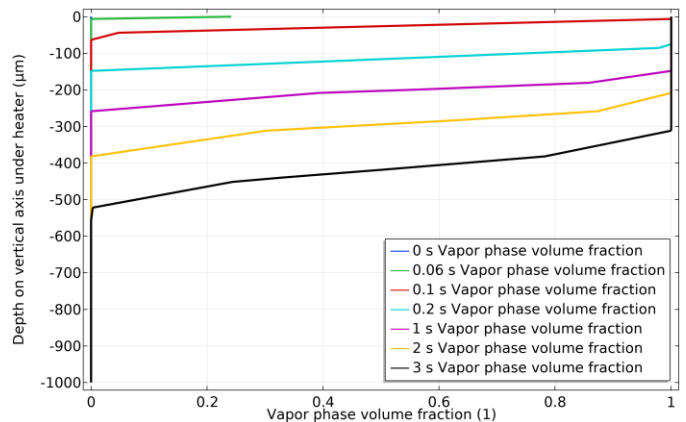


Figure 9 time-transient vapor volume fraction on vertical axis in wick.

Heat fluxes

Ideally, it is desired that all the input electrical power goes to the wick material for evaporation purposes, however in reality we experience heat losses to surrounding components. The electrical power input (blue line) is compared to heat losses to wick component, epoxy glue, ambient air, and copper pads through wire bonds in Figure 10. The biggest power losses are those to wick material and epoxy glue. Power loss through wire bonds and convection to air is negligible.

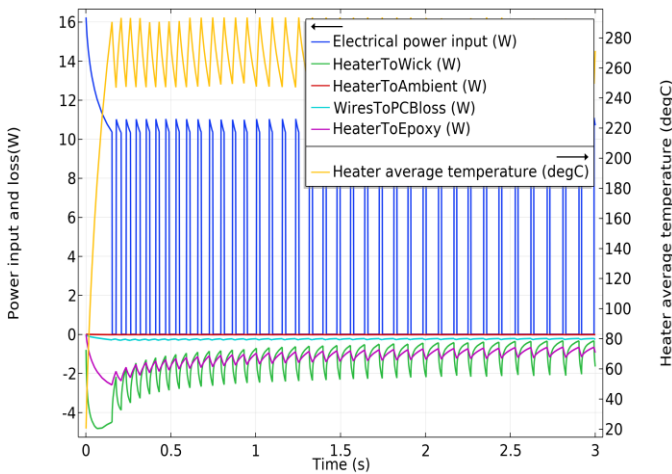


Figure 10 heater element power input, heat losses, and temperature.

It is easily seen in Figure 10 that the electrical power input decreases from initial 16W to around 10W as the heater temperature rises and leads to electrical resistivity growth. Meanwhile, during the first 0.2 seconds the losses to wick and epoxy rise, with the loss to wick being almost 2 times of that to epoxy. Considering the power input of around 10W, and losses of 4.5W and 2.5W at 0.15 seconds, there is a missing 3W power. This amount is stored in the heater to increase its temperature from room temperature to working temperature. The storage rate is plotted in Figure 11 by calculating the expression $\iiint \rho C_p \frac{\partial T_{avg}}{\partial t} dv$.

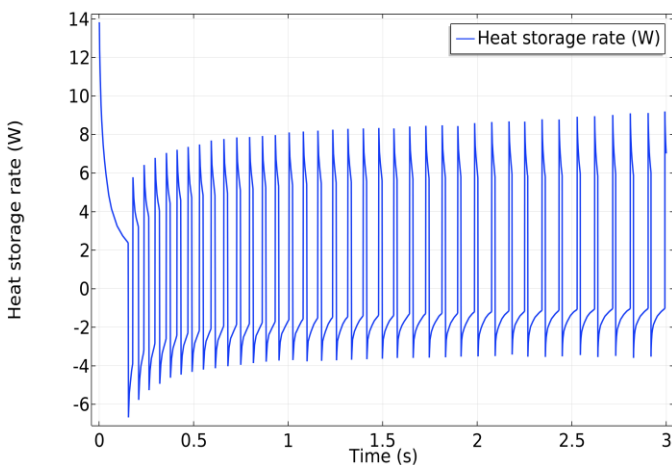


Figure 11 heat storage rate in the silicon heater element.

The storage energy rate is chosen over storage energy as it is comparable with other rates. The fluctuations in this value are due to the temperature regulation algorithm. Soon after evaporation starts, the losses to epoxy and wick start to get closer. It can be justified by the fact that the vapor layer has less heat conductivity than liquid and blocks the heat to wick.

Conclusions

Temperature distribution on the domain shows that the temperature on silicon heater, gold wire bonds and, copper is far below the melting temperature. On contrary, FR4 and epoxy are overheated. Epoxy damage is observed in some repetitive experiments, however, there is no PCB damage observed in all experiments. Vapor mass inside the wick after 3 seconds is about 0.65 mg when the heater is regulated around 270°C. Vapor is spread all beneath the heater, with more thickness in the middle. The vapor thickness under the middle point of the heater exceeds 0.3mm. Electrical power input, heat storage in wick, and heat losses align with energy conservation. Heat loss through wire bonds and convection with ambient is negligible. Most of the heat is conducted to wick material for evaporation and losses through epoxy. The loss through epoxy is almost half of that to the wick until 0.5 seconds of evaporation. After that, it is not interpretable due to temperature regulation fluctuations. The outflow is still not reflecting what happens in experiments. It might be because the gas density is considered more than the real one, due to convergence issues. True gas density is a thousand times less than that of liquid, which makes the phase change simulation challenging. Elaborating the mesh may help in this manner. There is also a neglected capillary force in the porous media. However, what is more important seems to be the evaporation model. Although the model describes pure material evaporation well, it is not accurate for mixtures. Investing more effort into the evaporation model is definitely worth it to make the results more aligned with experiments.

References

- [1] J. Pourchez, F. de Oliveira, S. Perinel-Ragey, T. Basset, J.-M. Vergnon, N. Prévôt, Assessment of new-generation high-power electronic nicotine delivery system as thermal aerosol generation device for inhaled bronchodilators, *International journal of pharmaceutics* 518 (2017) 264–269.
- [2] A.R. Bhashyam, M.T. Wolf, A.L. Marcinkowski, A. Saville, K. Thomas, J.A. Carcillo et al., Aerosol delivery through nasal cannulas: an in vitro study, *Journal of aerosol medicine and pulmonary drug delivery* 21 (2008) 181–188.
- [3] F. Goldschmidtboeing, U. Pelz, M. Ghanam, T. Bilger, A. Jamali, M. Saberi et al., Heater for Controlled Evaporation of Liquids for Personalized Drug Delivery to the Lungs, *J. Microelectromech. Syst.* (2020) 1–6.
- [4] Solving Models with Pulsed Loads in Time - Knowledge Base, [October 10, 2019], <https://www.comsol.com/support/knowledgebase/1245>.

Acknowledgments

The authors acknowledge the financial support of Hauni Maschinenbau GmbH to support the project.